Weekly Lab Meeting

Kyung Min Kwon

Nonlinear Optics and Photonics Device Lab
Department of Applied Physics
Kyunghee University

December 2, 2025

KHU NOPD LAB

Second order tensor - Impermeability tensor

A second-order tensor η_{ij} defined as the relation of an electric field and displacement field vector:

$$\eta_{ij} E_j = D_i \tag{1}$$

Index ellipsoid has the information of impermeability tensor.

Impermeability tensor is crystallographically given by:

$$\eta = \begin{pmatrix} 1/n_1^2 & 0 & 0 \\ 0 & 1/n_2^2 & 0 \\ 0 & 0 & 1/n_3^2 \end{pmatrix} \tag{2}$$

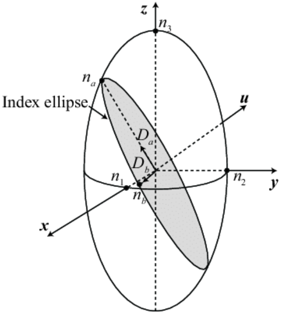

Second order tensor - Impermeability tensor

- **Transverse impermeability tensor**

  The intersection of the index ellipsoid with the $\mathbf{k} \cdot \mathbf{D} = 0$ plane.

- **The information of transverse impermeability tensor**

  Eigenvector of normal modes (eigenvector of transverse impermeability tensor) with their refractive index. (eigenvalues)

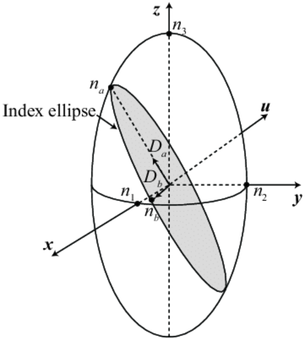

Pockels Perturbed Impermeability Tensor of PPKN

- **Periodically poled potassium niobate (PPKN)**

  A perovskite ferroelectric crystal belonging to the orthorhombic point group mm2 at room temperature.

  The crystallographic axes are labeled a, b, and c, with lattice parameters $a_0 = 5.6896$ Å, $b_0 = 3.9692$ Å, and $c_0 = 5.7256$ Å

  For $KNbO_3$ at $\lambda = 1550\ \mathrm{nm}$ and $T = 22^\circ\mathrm{C}$, the refractive indices are $n_a = 2.1975$, $n_b = 2.2321$, and $n_c = 2.1014$, obtained from Sellmeier equations.

  Assignment of dieelctric and crystallographic axes : $x, y, z \equiv b, a, c\,(2, 1, 3)$

  Quasi-phase-matched (QPM) devices in ferroelectric crystals are most commonly implemented using periodically poled 180° domains. Let [001] be $+c$ direction.

Pockels Perturbed Impermeability Tensor of PPKN

- **Pockels Perturbed Impermeability**

  A third-order tensor r_{ijk} defined as the linear derivative of the impermeability tensor with respect to the electric field: $\Delta\eta_{ij} = r_{ijk}E_k$

$$\eta_{ij}(\mathbf{E}) = \eta_{ij}(0) + \left.\frac{\partial \eta_{ij}}{\partial E_k}\right|_{\mathbf{E}=0} E_k + \frac{1}{2}\left.\frac{\partial^2 \eta_{ij}}{\partial E_k \partial E_\ell}\right|_{\mathbf{E}=0} E_k E_\ell + \cdots \tag{3}$$

  In our case, mm2 group is noncentrosymmetric. By using contracted notation, the Pockels term $r_{\mathrm{mk}}E_{\mathrm{k}}$ can be written explicitly as

$$r_{\mathrm{mk}}E_{\mathrm{k}} = \begin{pmatrix} 0 & 0 & \pm r_{13} \\ 0 & 0 & \pm r_{23} \\ 0 & 0 & \pm r_{33} \\ 0 & \pm r_{42} & 0 \\ \pm r_{51} & 0 & 0 \\ 0 & 0 & 0 \end{pmatrix} \begin{pmatrix} E_1 \\ E_2 \\ E_3 \end{pmatrix} = \begin{pmatrix} \pm r_{13}E_3 \\ \pm r_{23}E_3 \\ \pm r_{33}E_3 \\ \pm r_{42}E_2 \\ \pm r_{51}E_1 \\ 0 \end{pmatrix}. \tag{4}$$

Pockels Perturbed Impermeability Tensor of PPKN

- **Pockels Perturbed Impermeability**

  Unclamped : T, clamped : S

Pockels Tensor	r^T_{mk} [pm/V]	r^S_{mk} [pm/V]
r_{13}	34 ± 2	20.1 ± 2
r_{23}	6 ± 1	7.1 ± 0.5
r_{33}	63.4 ± 1	34.4 ± 2
r_{51}	120 ± 10	27.8 ± 3
r_{42}	450 ± 30	360 ± 30

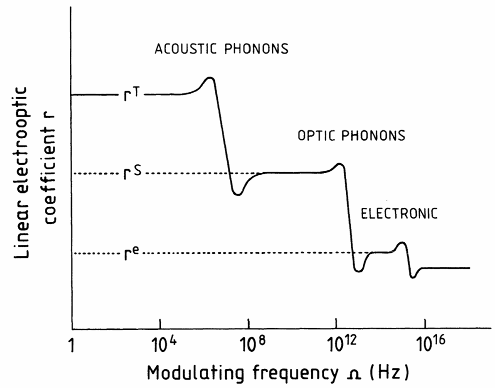

Pockels Perturbed Impermeability Tensor of PPKN

- **Pockels Perturbed Impermeability**

  The index ellipsoid of the crystal in the presence of an applied field

$$\eta(\mathbf{E}) = \eta(\mathbf{0}) + \mathbf{r}\,\mathbf{E} = \begin{pmatrix} \frac{1}{n_1^2} \pm r_{13}E_3 & 0 & \pm r_{51}E_1 \\ 0 & \frac{1}{n_2^2} \pm r_{23}E_3 & \pm r_{42}E_2 \\ \pm r_{51}E_1 & \pm r_{42}E_2 & \frac{1}{n_3^2} \pm r_{33}E_3 \end{pmatrix}. \tag{5}$$

  The magnitude of the Pockels term $r_{\mathrm{mk}}E_{\mathrm{k}}$ is typically on the order of 10^{-5}.

  $\rightarrow$ Treat as a small perturbation.

Modeling as EO Bragg Modulator

- **Bragg-regime criteria**

$$Q = \frac{2\pi\lambda L}{n\Lambda^2}, \qquad p = \frac{\lambda^2}{n\Delta n\Lambda^2}. \tag{6}$$

Δn : the effective refractive index contrast for anisotropic medium.

For Bragg regime, $Q \gg 1$ and $p \gg 1$.

Substituting Eqs. (2) and (3) in Eq. (1) and neglecting the second derivative with respect to z, we arrive at the well-known set of coupled wave equations:

$$\frac{\partial \phi_l}{\partial \xi} = j\rho l^2(1 - B_l)\phi_l + j(\phi_{l-1} + \phi_{l+1}), \tag{4}$$

where $B_l = 2\Lambda \sin\theta_0/\lambda_0 l$, θ_0 is the external angle of incidence, $\xi = \nu(z/L)$, $\nu = \pi n_1 L/\lambda_0 \cos\theta_1$, and θ_1 is the angle of diffraction of the zero-order mode. Thus, B_l is equal to 1 for Bragg diffraction forming the lth mode, and ν is a measure of the grating strength (and appears, e.g., in the coupled mode theory of Kogelnik for Bragg diffraction[3]). The absorption constant α may be neglected

Modeling as EO Bragg Modulator

- **Theoretical Description of EO Bragg modulator**

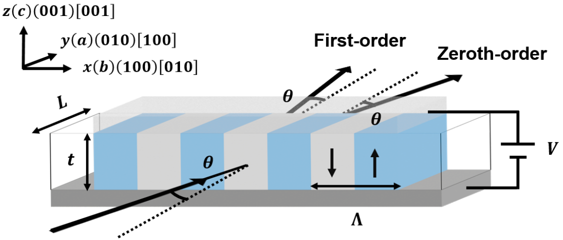

The grating vector : $\mathbf{K} = -(2\pi/\Lambda)\hat{\mathbf{x}}$

An applied field: $\mathbf{E} = (V/t)\,\hat{\mathbf{z}}$

The incident wavevector lies in the $x - y$ plane at an external angle θ measured from the y-axis.

Modeling as EO Bragg Modulator

- **Theoretical Description of EO Bragg modulator**

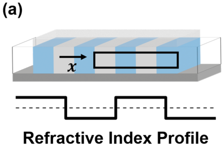

The square-wave grating :

$$\epsilon(x) = \epsilon^{(0)} + \sum_{\text{odd } m} \Delta\epsilon^{(m)} \cos(mKx), \tag{7}$$

The internal Bragg condition

$$\sin\theta_B = \frac{\lambda}{2n\Lambda}, \tag{8}$$

n:the refractive index of the polarization mode of 0th and 1st ordered wave.

The grating is effectively treated as:

$$\epsilon(x) \approx \epsilon^{(0)} + \Delta\epsilon^{(1)} \cos(Kx), \tag{9}$$

Modeling as EO Bragg Modulator

- **Theoretical Description of EO Bragg modulator**

The phase matching is already satisfied by the Bragg condition,

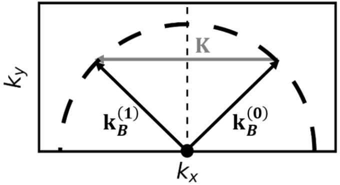

$$\Delta \mathbf{k} = \mathbf{k}_B^{(1)} - \mathbf{k}_B^{(0)} - \mathbf{K} = 0, \tag{10}$$

The zeroth-order and first-order Bragg wavevectors

$$\mathbf{k}_B^{(0)} = k(\sin\theta_B \hat{x} + \cos\theta_B \hat{y}), \tag{11}$$

$$\mathbf{k}_B^{(1)} = k\left(-\sin\theta_B \hat{x} + \cos\theta_B \hat{y}\right), \tag{12}$$

where $k = 2n\pi/\lambda$. The polarization mode of the incident and diffracted waves are same.

Modeling as EO Bragg Modulator

- **Eigenvectors of the unperturbed impermeability tensor**

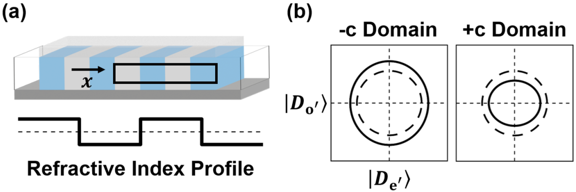

For Bragg-angle propagation in PPKN, the eigenvectors $|D_{o'}\rangle$ and $|D_{e'}\rangle$ of the transverse impermeability tensor are determined by the index ellipse, the intersection of the index ellipsoid with the $\mathbf{k}_B \cdot \mathbf{D} = 0$ plane.

Power splitting by superposition of two eigenvectors.

$\rightarrow$ Decreasing the diffraction efficiency

Modeling as EO Bragg Modulator

- **Eigenvectors of the unperturbed impermeability tensor**

  The eigenvectors with the condition $\mathbf{k}_B \cdot \mathbf{D} = 0$

$$|D_{o'}\rangle = \hat{x} \mp \tan\theta_{B,o'}\hat{y}, \tag{13}$$

$$|D_{e'}\rangle = \hat{z}. \tag{14}$$

  The eigenpolarizations of the normal modes with $\mathbf{E} = \boldsymbol{\eta}\mathbf{D}$.

$$|E_{o'}\rangle = \frac{1}{\sqrt{1+\beta^2}}\left(\hat{x} \mp \beta\hat{y}\right), \tag{15}$$

$$|E_{e'}\rangle = \hat{z}. \tag{16}$$

  where $\beta = (n_2^2/n_1^2)\tan\theta_{B,o'}$.

Modeling as EO Bragg Modulator

- **Eigenvectors of the unperturbed impermeability tensor**

  Their effective refractive indices are given by

$$\frac{1}{n_{\mathrm{o}'}^2} = \frac{\cos^2\theta_B}{n_2^2} + \frac{\sin^2\theta_B}{n_1^2}, \tag{17}$$

$$n_{\mathrm{e}'} = n_3. \tag{18}$$

  Small Bragg angle ($\theta_B \ll 1$)

  $\rightarrow$ zeroth-order $|E_{o'}^{(0)}\rangle$ and first-order eigenpolarization $|E_{o'}^{(1)}\rangle$ are nearly x-polarized, with their refractive index close to $n_{o'} \approx n_2$.

Modeling as EO Bragg Modulator

- **Spatial Beam Walk-off of the Unperturbed Impermeability Tensor.**

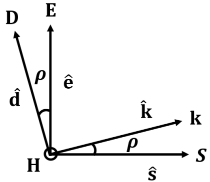

For a plane wave, **D**, **E**, **S**, and the wave normal **k** are coplanar.

$$\tan\rho = \frac{\hat{\mathbf{e}}\cdot\hat{\mathbf{s}}}{\hat{\mathbf{e}}\cdot\hat{\mathbf{d}}} = n^2\left[\left(\frac{k_x}{n^{-2}-n_2^{-2}}\right)^2+\left(\frac{k_y}{n^{-2}-n_1^{-2}}\right)^2+\left(\frac{k_z}{n^{-2}-n_3^{-2}}\right)^2\right]^{-1/2} \quad (19)$$

$(k_x,\, k_y\,,k_z)$: the components of the wavevector of the polarization modes (o' or e') along the principal axes

$n_1,\, n_2,\, n_3$: refractive indices of crystallograpic axes of the polarization modes.

Modeling as EO Bragg Modulator

- **Spatial Beam Walk-off of the Unperturbed Impermeability Tensor.**

  Under the Bragg condition, $\mathbf{k_B} = k\left(\pm\sin\theta_B\hat{x} + \cos\theta_B\hat{y}\right)$

$$\tan\rho_{o'} = n_{o'}^2\left[\left(\frac{\sin\theta_{B,o'}}{n_{o'}^{-2} - n_2^{-2}}\right)^2 + \left(\frac{\cos\theta_{B,o'}}{n_{o'}^{-2} - n_1^{-2}}\right)^2\right]^{-1/2}. \tag{20}$$

  In our case, where the propagation vector lies in the x–y plane, the e'-polarized mode exhibits no beam walk-off, since $\hat{\mathbf{e}}\cdot\hat{\mathbf{d}} = 0$.

Analytic Expression

- **Coupled Wave Theory for Anisotropic Thick Hologram Theory**

A further simplification is obtained in the case of perfect Bragg matching ($\Delta \vec{k}_r = \vec{0}$, $\xi^2 = 0$). In this case Eq. (39) becomes

$$\eta(d) = \sin^2\left(\frac{\pi A_r d}{2\lambda(n_s n_p g_s g_p \cos\theta_s \cos\theta_p)^{1/2}}\right) e^{-2\alpha d}, \tag{41}$$

where λ is the vacuum wavelength. The argument of the sin function is of the form $(\pi \Delta n d/\lambda \cos\theta)$ in analogy with Ref. [1], with $\Delta n = A_r/[2(n_s n_p g_s g_p)^{1/2}]$ and $\cos\theta = (\cos\theta_s \cos\theta_p)^{1/2}$. In nonabsorbing materials the maximum

Analytic Expression

- **Coupled Wave Theory for Anisotropic Thick Hologram Theory**

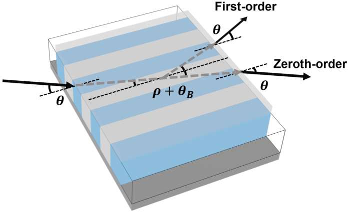

The First-order diffraction efficiency at $y = L$ under the perfect phase matching,

$$\eta_d(L) = \sin^2\left(\frac{\pi \Delta n L}{\lambda \cos(\theta_B - \rho)}\right), \tag{21}$$

The effective index contrast Δn for an anisotropic medium

$$\Delta n = \frac{\langle E^{(1)} | \Delta\epsilon^{(1)} | E^{(0)} \rangle}{2n\cos\rho}. \tag{22}$$

Here, $\theta_i = \theta_B = -\theta_d$ in the Bragg configuration.

Analytic Expression

- **Coupled Wave Theory for Anisotropic Thick Hologram Theory**

  the dielectric contrast $\Delta\epsilon$ to the first Fourier component $\Delta\epsilon^{(1)}$ of the square-wave grating

$$\Delta\epsilon^{(1)} \approx -\frac{2}{\pi}\epsilon\left(\mathbf{0}\right)\Delta\eta\,\epsilon\left(\mathbf{0}\right) \tag{23}$$

  where unperturbed dielectric tensor $\epsilon\left(\mathbf{0}\right) = \left(\eta\left(\mathbf{0}\right)\right)^{-1}$.

Analytic Expression

- **180°-domain PPKN**

  The contrast of the impermeability tensor

$$\Delta\eta = \begin{pmatrix} 2r_{13}E & 0 & 0 \\ 0 & 2r_{23}E & 0 \\ 0 & 0 & 2r_{33}E \end{pmatrix} \tag{24}$$

  The first-order Fourier component of the dielectric tensor modulation

$$\Delta\epsilon^{(1)} = -\frac{2}{\pi} \begin{pmatrix} 2n_1^4 r_{13}E & 0 & 0 \\ 0 & 2n_2^4 r_{23}E & 0 \\ 0 & 0 & 2n_3^4 r_{33}E \end{pmatrix} \tag{25}$$

Analytic Expression

- **o'-polarized wave of 180°-domain PPKN**

  Diffraction efficiency

$$
\begin{aligned}
\eta_d(L) &= \sin^2\!\left[\frac{2}{1+\beta^2}\,\frac{L\,(n_2^4\,r_{23}-\beta^2 n_1^4 r_{13})\,V}{\lambda\,t\,n_{o'}\cos(\theta_B-\rho_{o'})\cos\rho_{o'}}\right] \\
&\approx \sin^2\left[\frac{2L\,n_2^3\,r_{23}\,V}{\lambda\,t\cos(\theta_B-\rho_{o'})\cos\rho_{o'}}\right].
\end{aligned}
\tag{26}
$$

  Half-wave voltage V_π

$$
\begin{aligned}
V_\pi &= \frac{(1+\beta^2)\pi\,n_{o'}\lambda\,t\,\cos(\theta_B-\rho_{o'})\cos\rho_{o'}}{4L\,n_2^4\,r_{23}} \\
&\approx \frac{\pi\,\lambda\,t\,\cos(\theta_B-\rho_{o'})\cos\rho_{o'}}{4L\,n_2^3\,r_{23}}.
\end{aligned}
\tag{27}
$$

Analytic Expression

- **e'-polarized wave of 180°-domain PPKN**

  Diffraction efficiency

$$\eta_d(L) = \sin^2\left[\frac{2L\, n_3^3\, r_{33}\, V}{\lambda\, t \cos\theta_B}\right]. \tag{28}$$

  Half-wave voltage V_π

$$V_\pi = \frac{\pi\, \lambda\, t \cos\theta_B}{4L\, n_3^3\, r_{33}}. \tag{29}$$

Benchmarking Results with RCWT

- **Setting physical device parameter**

Table 2: Reported fabrication parameters of bulk 180°-domain PPKN devices, reformulated for the EO Bragg modulator considered in this work. In this convention, the crystal thickness t is along the c axis, whereas the interaction length L is defined along the a axis.

Thickness t (mm)	Length L (mm)	Poling period Λ (μm)	Reference
0.925	3	32.5	Kim & Yoon, Appl. Phys. Lett. **81**, 3332 (2002) [24]
1.0	10	35.5	Hirohashi *et al.*, Jpn. J. Appl. Phys. **43**, 559 (2004)[25]
1.0	8	14.4	Yu *et al.*, Appl. Phys. Lett. **85**, 5839 (2004) [26]
1.0	10	30	Meyn *et al.*, Opt. Lett. **24**, 1154 (1999) [27]

This thickness is consistent with domain measurements on a 0.6 mm-thick c-cut $KNbO_3$ plate, we adopt 0.5 mm in our simulations.

A crystal length $L = 1\ \mathrm{cm}$, a crystal thickness $t = 500\ \mu\mathrm{m}$, and a poling period $\Lambda = 14.4\ \mu\mathrm{m}$ at an operating wavelength of $\lambda = 1550\ \mathrm{nm}$.

Benchmarking Results with RCWT

- **Anti-reflection coating (single layer AR coating)**

  For so small Bragg angle, the incident wave is close to normal.

  The thickness $t_f = \lambda/(4n_f)$, where $n_f \approx \sqrt{n_{\mathrm{air}} n_j}$ for $j = o', e'$.

  This design value is close to that of SiO_2 with $n_f = 1.4431$, yielding a film thickness of $t_f \approx 268$ nm at $\lambda = 1550$ nm.

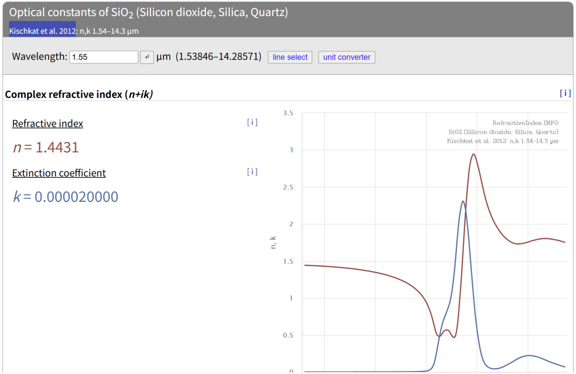

Good Convergence

$L = 1$ cm, $t = 500$ μm, $\Lambda = 14.4$ μm and $\lambda = 1550$ nm

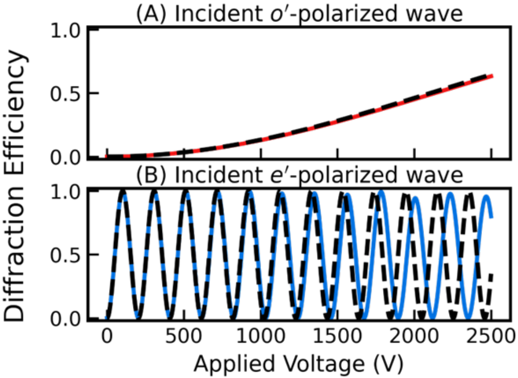

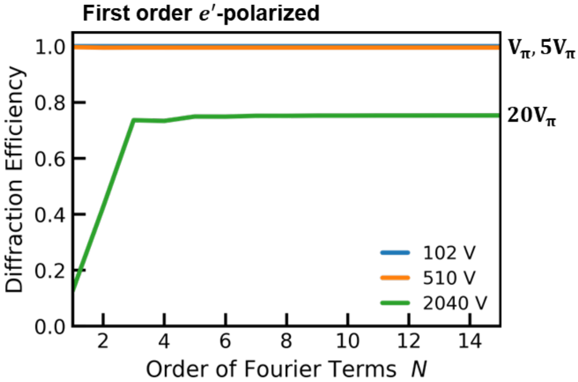

As the applied voltage increases (the refractive index contrast increases), the period ($\sin^2$) of the diffraction efficiency becomes longer and higher-order Fourier components redistribute the diffraction efficiency.

Numerical results

external incidence angle in air :3.085°

internal incidence angles of 1.468° and 1.382° for the o'- and e'-polarized waves, respectively.

The beam walk-off angle of the o'-polarized wave, $\rho_{o'} = 0.0439^\circ$

The e'-polarized wave exhibits no beam walk-off.

Bragg or not?

$Q = 210.4$ and $Q = 223.5$ for o'-polarized and e'-polarized incidence, respectively.

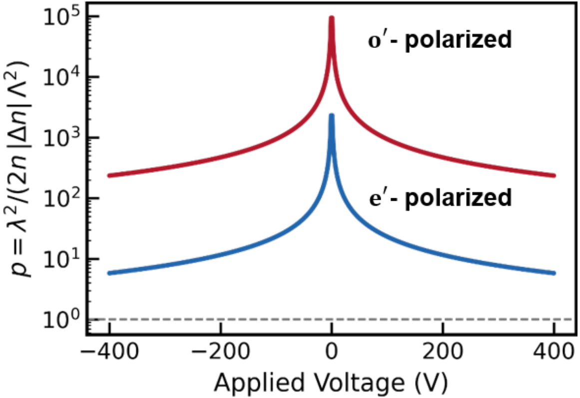

These results indicate that the applied voltage controls the contrast of effective refractive index and that p decreases as the voltage increases.

RCWT vs anisotropic Thick hologram theory

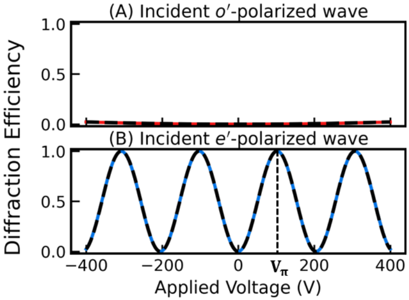

r_{33} of e'-polarized wave

$\rightarrow$ In unclamped $KNbO_3$, r_{33} is approximately twice that of congruent $LiNbO_3$ (Li/Nb $=$ 0.937), while their principal refractive indices are comparable ($n_3 \approx 2.10$ for $KNbO_3$ and $n_e \approx 2.14$ for $LiNbO_3$).

The half-wave voltage V_π of the EO PPLN Bragg modulator can be expected to be roughly half that of a comparable PPLN device.

Conclusion

(1) The half-wave voltage V_π of the EO modulator in $KNbO_3$ can be expected to be roughly half that of a comparable PPLN device.

(2) When the Bragg angle or beam walk-off cannot be neglected, the full anisotropic expressions derived in this work must be used.

$\rightarrow$ The analytic expressions derived in this work can be directly applied to many other periodically poled ferroelectric crystals, our analysis naturally extends beyond PPKN devices.